



The Society shall not be responsible for statements or opinions advanced in papers or in discussion at meetings of the Society or of its Divisions or Sections, or printed in its publications. Discussion is printed only if the paper is published in an ASME Journal or Proceedings. Released for general publication upon presentation. Full credit should be given to ASME, the Technical Division, and the author(s).

Copyright © 1981 by ASME

A Theory for Fine Particle Deposition in 2-D Boundary Layer Flows and Application to Gas Turbines

M. Agengiitürk

Associate Professor,
Department of Mechanical Engineering,
Bogazici University,
Istanbul, Turkey

E. F. Sverdrup

Advisory Engineer,
Westinghouse Research & Development
Center,
Pittsburgh, Pa.

A theory is presented to predict deposition rates of fine particles in two-dimensional compressible boundary layer flows. The mathematical model developed accounts for diffusion due to both molecular and turbulent fluctuations in the boundary layer flow. Particle inertia is taken into account in establishing the condition on particle flux near the surface. Gravitational settling and thermophoresis are not considered. The model assumes that the fraction of particles sticking upon arrival at the surface is known, and thus, treats it as a given parameter. The theory is compared with a number of pipe and cascade experiments, and a reasonable agreement is obtained. A detailed application of the model to a turbine is also presented. Various regimes of particle transport are identified, and the range of validity of the model is discussed. An order of magnitude estimate is obtained for the time the turbine stage can be operated without requiring cleaning.

INTRODUCTION

When a gas stream containing fine particles flows over a surface, particles are deposited by various mechanisms. If the flow is laminar, particles are diffused toward the surface by Brownian motion. The particle flux normal to the surface is, then, given by

$$N = -p D_B \frac{dC}{dy} \quad (1)$$

where C is the particle relative concentration, p fluid density, and y coordinate normal to the surface. The Brownian diffusion coefficient, D_B , is given by the Einstein formula [1]

$$D_B = \frac{K_B T}{3\pi\eta d} \quad (2)$$

where T is the fluid temperature, η viscosity, K_B Boltzmann constant, and d particle diameter.

Deposition in turbulent boundary layer flows can be envisioned as a diffusion process which is highly intensified by turbulent fluctuations. Unless the particles are extremely small, the resulting particle diffusivity can be several orders of magnitude greater than in the case of molecular (Brownian) diffusion alone. The particle flux in such flows can be written as follows

$$N = -p (D_B + D_T) \frac{dC}{dy} \quad (3)$$

The additional coefficient, D_T , represents the contribution by the turbulent fluctuations and is called the eddy diffusivity of the particle.

If the diffusion coefficient and the continuity requirements on the particle flux are known in addition to the free stream concentration, the concentration profile inside the boundary layer can be calculated, and then, the particle arrival rate can be determined by evaluating Equation (3) at the surface. Upon reaching the surface, some of the particles stick and some are thrown back depending on the nature of attachment and detachment forces developing near the surface. The theory presented in this paper calculates the particle arrival rates. Calculation of the net deposition rates requires additional work to account for the reentrainment due to particle removal from the surface.

The present theory has direct application in the gas turbine industry. It can be used to predict the deposition rates in turbines expanding "dirty" gas. In its present form with assumptions or experimental measurements to establish the fraction of particles which stick on arrival or when the theory is extended to calculate the particle reentrainment, it allows one to set the tolerance level on particles that can be safely directed through the turbine, and therefore, to specify the degree of gas cleaning required for reliable turbine operation.

A few investigations of particle deposition in turbines have appeared in the literature. Parker and Lee [2] studied deposition of submicron particles on turbine blades. They used a theory developed by Lin, et al. [3] for turbulent flow in pipes which neglects the streamwise variation in velocity and concentration and neglects also the effect of particle inertia on diffusion. Consequently, their calculation displayed considerable discrepancy from their experimental results. Moore and Crane [4] calculated diffusive deposition rates for the suction surface of a representative blade profile, again by using a pipe flow model.

Contributed by the Gas Turbine Division of THE AMERICAN SOCIETY OF MECHANICAL ENGINEERS for presentation at the Gas Turbine Conference & Products Show, March 9-12, 1981, Houston, Texas. Manuscript received at ASME Headquarters December 9, 1980.

Copies will be available until December 1, 1981.

Crane [5] reported predictions of fog deposition on low pressure steam turbine blades. He concluded that deposition rates could not be estimated accurately unless the real compressible flow over the curved blade surfaces was considered. The theory presented here aims at closing the existing gap and at furnishing the engineer with a reliable tool to predict fine particle arrival rates in turbines.

THEORY OF DIFFUSIVE PARTICLE TRANSPORT

Particle Transport Equation

A two dimensional compressible flow is considered over a surface of arbitrary shape. The flow geometry and the coordinate system are shown in Figure 1. The x-coordinate is the surface distance measured from the leading edge; the y-coordinate is measured normal to the surface.

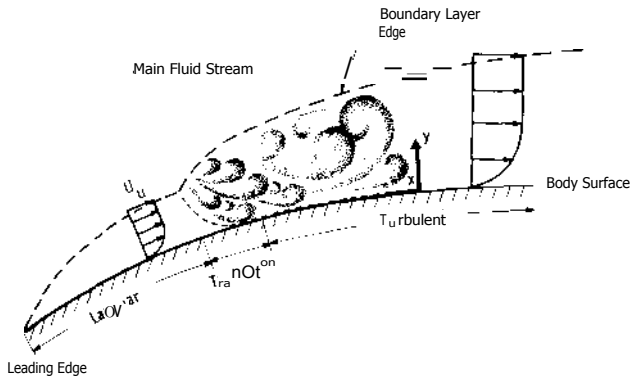


Fig. 1 The flow geometry and the coordinate system

The particle content of fluid is given by the particle concentration, c , which is assumed to be small enough so that the fluid properties are unaffected by the presence of particles. It is also assumed that particles are small enough so that purely inertial deposition is negligible. In other words, particle deviation from gas streamlines is small, and thus, deposition occurs mainly by diffusion. Particle inertia will be taken into account in establishing the condition on the particle flux near the surface. Gravitational effects are neglected.

The continuity requirement for steady particle flow may be expressed by the following mass transfer equation [6]

$$\frac{d}{dx} (p D_p \frac{dc}{dx}) + \frac{d}{dy} (p c v) = 0 \quad (4)$$

where v is the velocity and D_p is the isotropic diffusion coefficient. The relative particle concentration, χ , is defined as c/p .

Neglecting diffusion in x-direction and defining a stream function, G , Equation (4) becomes

$$\frac{d}{dy} (p D_p \frac{d\chi}{dy}) - \frac{DG}{By} = \frac{3G}{Dx} \frac{DIP}{By} \quad (5)$$

where $u = (1/p) (BG/Dy) = x$ -component of velocity.

$$v = (-1/p) (DG/3x) \quad \text{y-component of velocity.}$$

The diffusion coefficient may be written as

$$D_p = D_B + D_T \quad (6)$$

where D_T , the eddy diffusivity, may be expressed as the sum $E_f + E_p$, E_f being the eddy viscosity and C ; denoting the correction factor for particle size. Using the expression given by Liu and Ilori [7] for C and Equation (1) for D_B , the diffusion coefficient takes the form

$$D_p = \frac{K T}{371.1 d_p} + E_f + \frac{1}{18} \frac{p d_p^2 T^2}{U (y + 1011)^2} \quad (7)$$

where P_p is the particle density and τ_w is the shear stress at the surface.

The eddy viscosity, E_f , can be represented by a two layer model. The eddy viscosity for the inner region is given by

$$E_{f1} = K_1 \frac{u_\tau^2}{y} \{ 1 - \exp[- \frac{y}{\delta} (\frac{u_\tau}{u_\tau^*} + \frac{dx}{d}) \frac{1}{2}] \}^2 \quad (8)$$

The eddy viscosity in the outer region is expressed as

$$E_{f2} = K_2 u_\tau \delta [1 - 5.5 (y/\delta)^6]^{-1} \quad (9)$$

where u_τ is the velocity at the outer edge of the boundary layer, δ boundary layer thickness, δ_d displacement thickness and τ_w shear stress at the surface.

Equations (8) and (9) include the modifications suggested by Van Driest [8], Cebeci, et al. [9], and Klebanoff [10]. Following the suggestion by Cebeci, et al. [9], the inner and outer regions are defined by the constraint of continuity in the eddy viscosity. Starting from the surface, Equation (8) is used until $E_{f1} = E_{f2}$, and then, Equation (9) applies. The choice of constants K_1 and K_2 depends on the definition of the boundary layer thickness, δ . If δ is defined as the y-distance where the velocity reaches 99.5% of the velocity outside the boundary layer, then $K_1 = 0.4$ and $K_2 = 0.0168$.

Transportation of Particle Transport Equation

When velocities in the boundary layer are known analytically or from a numerical computer solution, Equation (5) is a linear second order partial differential equation for χ . A direct solution is impossible, because the equation contains a singularity at the origin.

The singularity in the x-y plane can be removed by a transformation into the Levy-Lees plane defined by the η and p coordinates. The Levy-Lees transformation [11] is written here as

$$\eta = \int_0^x u dx \quad (10)$$

$$\chi = \int_0^y \frac{p u}{\tau_w} dy \quad (2)$$

where the subscript u denotes values at the outer edge of the boundary layer.

The partial derivative operators are transformed into the new plane according to

$$\frac{\partial}{\partial x} = \frac{\partial}{\partial \xi} + \frac{an}{DE} \frac{\partial}{\partial \eta} \quad (12)$$

$$\frac{\partial}{\partial y} = \frac{P_{uu}}{(2E)^{1/2}} \frac{\partial}{\partial \eta} \quad (13)$$

For convenience, a dimensionless stream function, $f(\xi, \eta)$, is related to $G(x, y)$ as follows [9]

$$f = \frac{P_{uu}}{(2E)^{1/2}} \xi \eta \quad (14)$$

After substituting Equations (12) through (14) into Equation (5),

$$\frac{D^2 z}{3n^2} + \left(\frac{2}{p} \frac{DP}{an} + \frac{1}{D} \frac{P^2}{pp} + \frac{A}{p^2 Dp} \right) \text{ of } \left(\frac{Bf}{p^2 pp} + \frac{D}{p^2 pp} - \frac{A}{p^2 pp} - \frac{3f}{D} \right) \quad (15)$$

where

$$A = gp_p u_a \quad (16)$$

$$B = p_u p_a \quad (17)$$

Boundary Conditions

The particle transport equation in the $\xi - \eta$ plane (Equation 15) can be solved when the conditions on η and/or its first derivative are specified at the outer edge of the boundary layer and at the surface.

The upper boundary condition requires the normal gradient of relative concentration to vanish at infinity. For numerical calculations it is appropriate to approximate this condition as

$$\frac{\partial V}{\partial \eta} \Big|_{\eta=h^*} = 0 \quad (18)$$

Here, h^* is a finite but sufficiently great distance in the η -direction. In many situations it is adequate to take $h^* = 6^*$ where 6^* is the boundary layer thickness in the $\xi - \eta$ plane.

The lower boundary condition requires additional considerations. Depending on the particle size and the flow conditions, there exists a certain distance measured from the surface within which diffusion alone is insufficient to represent the transport phenomenon. Particles coming that close to the surface need only a small impetus to reach the surface. It has been proposed by Friedlander and Johnstone [12] that this impetus is provided by the particle inertia. According to their stopping distance theory, particle transport toward the surface occurs by diffusion until the stopping distance from the surface; particles are considered to complete the final phase of their travel by way of a free flight (inertial coasting) which takes place under the momentum imparted by turbulent fluctuations and molecular motions. By assuming Stokes

flow and taking into account the particle radius in the manner suggested by Davies [13], the particle stopping distance may be calculated from the following equation

$$p_p \frac{dv_s}{ds} = \frac{d}{2} \quad (19)$$

where s is the stopping distance and v_s denotes the free flight initial velocity. As Beal [14] points out, v_s may be determined by summing the Brownian velocity due to molecular motions and the r.m.s. normal fluctuating velocity at the stopping distance. The Brownian velocity is given by [14]

$$v_B = \frac{1}{k} \frac{3kT}{72p_p} \frac{D}{p_p} \quad (20)$$

The r.m.s. normal fluctuating velocity, v_{a_s} , can be obtained from Davies correlation [13]

$$v_{a_s} = \frac{Y T_w}{10p_p} \quad (21)$$

From Equations (20) and (21) the normal particle velocity at a point near the surface may be written as

$$v_p = \left(\frac{3kT}{72p_p} \frac{D}{p_p} \right)^{1/2} + \frac{Y T_w}{10p_p} \quad (22)$$

The stopping distance is calculated by substituting v_s in Equation (22) and solving the resulting expression for v_s and Equation (19) by iteration. The normal particle flux at the stopping distance can be obtained from the concentration gradient at that point

$$N_s = -p D_p \frac{\partial c}{\partial y} \Big|_{y=s} \quad (23)$$

For simplicity the particles crossing into the inertial region are assumed to be transported to the wall at an average velocity v_c which is obtained by averaging the particle velocity over the stopping distance.

$$v_s = \frac{\int_0^s v_p dy}{s} \quad (24)$$

Since some of the particles do not quite reach the surface, and some do not stick on impact, Beal [14] postulates that there will be an equilibrium concentration, IP_s , within the stopping distance (inertial region). Thus, the flux of particles reaching the surface is

$$N_w = - \frac{v_c}{2} p c c_s \quad (25)$$

where p_c is the fraction of the particles which stick on impact. The average velocity is to be halved because there is equal probability of particles being thrown back toward the main stream.

Since $4) = 1P_s$ in the inertial region, $N_w = N_s$. Hence, combining Equations (23) and (25)

$$\rho_s \frac{2}{v_e} \frac{DTP}{c_8 Y Y's} \quad (26)$$

Equations (17) and (24) can be transformed into the $E - n$ plane as follows

$$s^* - \frac{u}{(2)^{1/2}} \int P^d Y \quad (27)$$

$$\rho_s \left[(20 \ 12 \ v_c p_c \ D r \ I \ n's^* \right] \quad (28)$$

Equation (28) is the lower boundary condition of the particle transport equation. A schematic illustration of the boundary conditions is given in Figure 2.

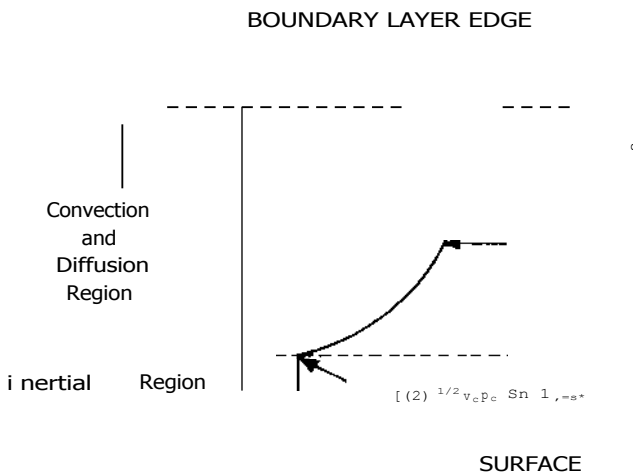


Fig. 2 Schematic illustration of the boundary conditions

Numerical Solution of the Particle Transport Equation

Equation (15) is a second order linear partial differential equation. The fluid properties and velocities that appear in the coefficients are known as a function of position from an analytical or numerical solution of the boundary layer flow. The remaining parameters can be calculated from this flow field.

A two dimensional five point mesh is used for the finite difference solution of Equation (15). By using Lagrange's interpolation method, the $\frac{\partial}{\partial x}$ and $\frac{\partial}{\partial y}$ derivatives are expressed in a finite difference form. The flow surface is divided into a number of stations which constitute the streamwise mesh points. At the leading edge the flow is laminar, but it may become turbulent at the subsequent stations depending on the flow conditions. The finite difference equation is solved at each surface station by making use of the boundary conditions and the solution at the previous stations. The solution is thus marched out in the streamwise direction. The particle transport equation in the "stretched" $E - n$ plane implicitly accounts for the conditions at the leading edge. Hence, when solution for the entire boundary layer is sought, there is no need to specify an initial concentration profile.

However, if solution is to be started at any other location, the corresponding initial profile must be given.

COMPARISON WITH EXPERIMENTS

Pipe Flow

In comparing the theory with pipe experiments, the particle transport equation may be greatly simplified by assuming incompressible flow and neglecting the change of the velocity and the concentration profiles in the axial direction. If it is further assumed that the diffusion thickness is much smaller than the pipe radius, Equation (15) reduces to

$$D \frac{d^2 c}{dy^2} = K_p c \quad (29)$$

This equation was solved by using the method described above. The upper boundary was taken at $h = 30(11/\rho u^*)$, where u^* is the friction velocity and the sticking fraction was assumed to be 1. The results are presented in terms of the deposition velocity, K_p , defined as

$$K_p = N \frac{w}{c_m}$$

where c_m is the mean concentration in pipe.

Comparison of the theoretical results with Friedlander and Johnstone's data [12] and Wells and Chamberlain's data [15] is shown in Figures 3 and 4, respectively.

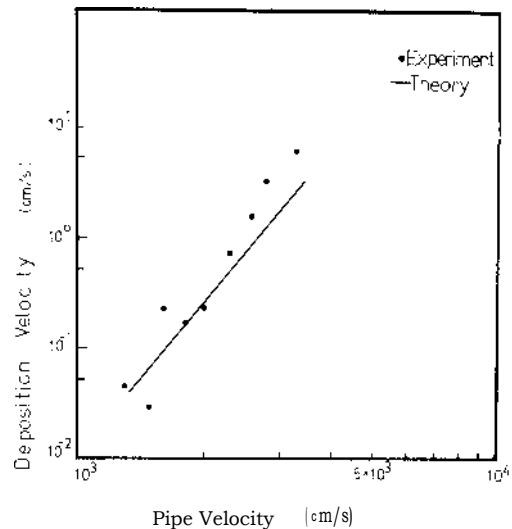


Fig. 3 Comparison with Friedlander and Johnstone's [12] experiments (1,81 pm aluminum particles in 1.38 cm pipe)

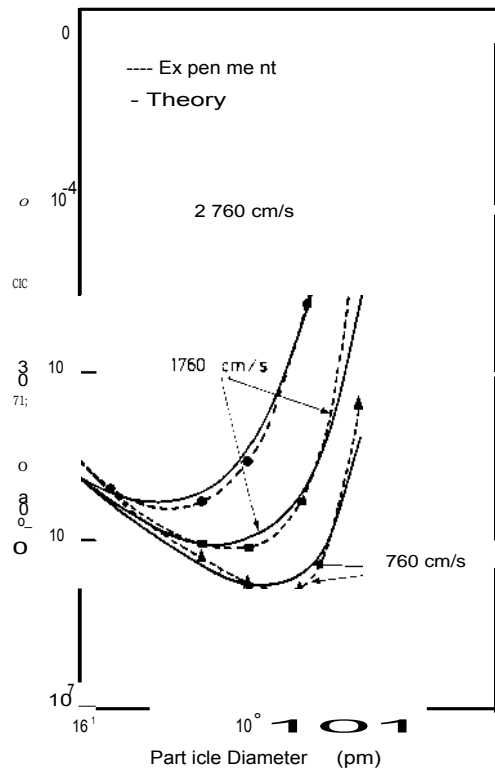


Fig. 4 Comparison with Wells and Chamberlain's [15] experiments (aitken nuclei, drops of tricresyl phosphate and polystyrene spheres at three different velocities in 2.54 cm pipe)

Cascade Flow

Comparison with pipe experiments hardly provides a rigorous verification for all aspects of the model. For a more complete test Parker and Lee's experiments [2], [16] in a two dimensional cascade were considered. The cascade geometry and the flow data are described by Parker and Lee. The measured surface velocities were used in the computer program E7ES by Cebeci, et al. [9] to calculate the velocities in the blade boundary layer. The sticking fraction was again assumed to be 1. The calculated deposition rates per cm^2 and the experimental data for 0.13 μm , 0.19 μm and 0.24 μm mass-median diameter fluorescein particles along the suction surface are shown in Figure 5. Here, the percentage deposition per cm^2 signifies the percentage deposition of particles passing through the blade passage in a zone 1 pitch wide by 1 cm deep. Since the flow rate was not given directly, it had to be calculated from the free stream velocities and the geometry. A consistent assessment was difficult. Therefore, the theoretical deposition rates were based on two values of the flow rate one calculated from the inlet velocity ($11500 \text{ cm}^3/\text{sec}$ per cm depth) and the other from the exit velocity ($17300 \text{ cm}^3/\text{sec}$ per cm depth). In view of this uncertainty, the theoretical results compare with the experiments quite well. Correlation would be improved if the size distribution had been available for each sample and had been taken into account in calculations instead of just using the mass-median diameters reported by Parker and Lee.

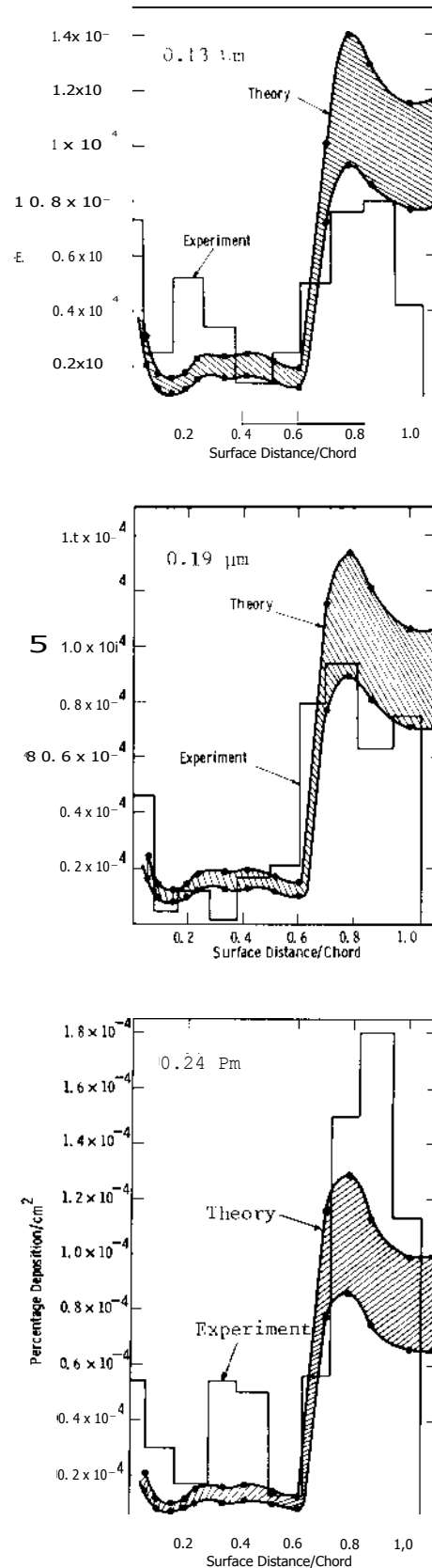


Fig. 5 Comparison with Parker and Lee's [2] Cascade experiments (0.13 μm , 0.19 μm and 0.24 μm fluorescein particles along blade suction surface)

The diffusive particle transport theory presented in this paper was applied to the first stage of an electric utility turbine rated to drive a 70 MW generator. The flow calculations were done by using the computer programs of Katsanis [17] and Cebeci, et al. [9]. The location of transition was calculated by applying the following criterion due to Horlock [18].

$$(Re_{\theta})_{transition} = \frac{U \theta}{\nu} = 250 \tag{31}$$

where θ is the local momentum thickness.

Results were obtained for particle with density of 2.5 gm/cc and diameters ranging from 0.001 μ m (- molecular size) to 3 μ m. It was assumed that all particles which arrived at the surface would stick ($p_c = 1$). The removal of deposits by the lift forces acting near the surface has not been considered. In these respects, the results presented in this paper are the rates of particle arrival at the surface rather than the actual deposition rates.

Based on the numerical results it is possible to distinguish three basic regimes of particle transport.

1. Brownian (Molecular) Diffusion Regime:

This regime is characterized by extremely small particles that are transported to surface mainly by Brownian (molecular) diffusion. Since the Brownian coefficient is inversely proportional to the particle diameter, the transport rate increases as the particle size decreases.

2. Turbulent Diffusion Regime:

This regime describes the transport of larger particles which diffuse under the influence of turbulent fluctuations. Since turbulent diffusion is enhanced by particle inertia, the transport rate increases as the particle diameter increases.

3. Inertial Regime:

In this regime particle momentum is more important than diffusion, Particle transport to surface occurs by direct inertial impaction. The present theory neglects the deviations of the particles from the main streamlines. Account is taken of the particle inertia only in the final "inertial coasting". Therefore, the transport theory presented in this paper cannot calculate the deposition rates in this regime accurately. Instead, one needs to trace the particle trajectories inside the boundary layer and to determine the amount of particles reaching the surface. A method of doing this is presented by Mengitirk and Sverdrup [19].

There certainly exist overlapping regimes in which a combination of various mechanisms is in effect. For example, in a mixed Brownian turbulent diffusion regime where S is negligible (See Equation 6), the transport rate will decrease as the particle size increases, since D_p is inversely proportional to d_p but of is independent of it.

The particle arrival rates will be presented in terms of the deposition velocity defined as

$$K_p = \frac{N_{arr}}{c_{in}} \tag{32}$$

where c_{in} is the particle concentration at the turbine inlet. The local arrival rate can be obtained by multiplying the deposition velocity by the inlet concentration.

Figures 6 and 7 show the calculated surface velocities and the boundary layer thicknesses, respectively, for the stator blades.

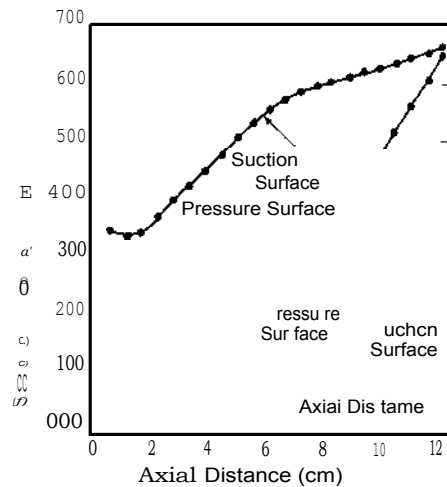


Fig. 6 Calculated surface velocities of stator blades

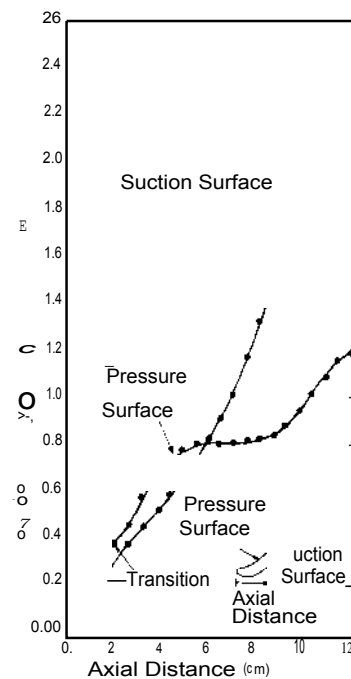


Fig. 7 Calculated boundary layer thicknesses of stator blades

The deposition velocities for 0.001 μm particles depositing on the pressure and suction surfaces of a stator blade are shown in Figure 8. It is seen that the deposition velocity decreases between the leading edge and the locations of transition on both surfaces. This is attributed to the increase in the boundary layer thicknesses. There is a marked increase in the deposition velocity at transition indicating the significance of turbulence. After transition the deposition velocity along the suction surface decreases steadily towards the leading edge owing to the rapidly thickening boundary layer. On the pressure surface it continues to increase at first (since the velocity is increasing but the thickness almost remains constant), then starts decreasing (since the effect of acceleration is offset by increasing thickness). It may be concluded that the velocity effect is not strong. The transport regime is Brownian diffusion in the laminar regions and a mixed Brownian-turbulent diffusion in the turbulent regions.

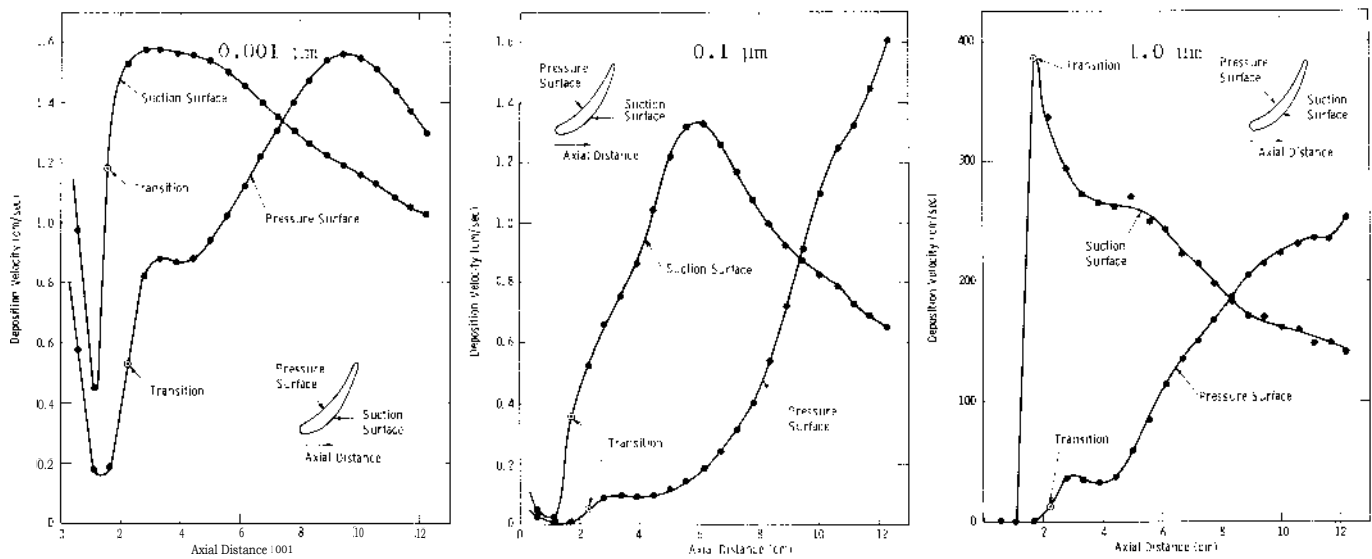


Fig. 8 Deposition velocities of 0.001 μm , 0.1 μm and 1.0 μm particles on stator blades

The change in the trend of the deposition velocities for 0.1 μm particles is readily observed. Transition causes more than an order of magnitude increase in deposition. The prevailing effect of turbulence is also reflected in the rest of the curves. Acceleration can, now, impressively oppose the retarding effect of boundary layer thickening on the transport rate. On the suction surface deposition velocities increase approximately midway to the trailing edge and only then begin to fall down. On the pressure surface the transport rates keep increasing all the way to the trailing edge. The transport regime is again Brownian diffusion in the laminar regions but entirely turbulent diffusion in the turbulent regions.

The deposition velocities for 1 μm particles exhibit further changes in the trend. The Brownian effect is virtually zero. On the other hand, the velocity effect characterizing the turbulent diffusion regime is somewhat underestimated, as evidenced by the variation of the calculated deposition velocity along the suction surface. For 1 μm particles, the stopping distance becomes comparable to the boundary layer thickness and the velocity at the stopping distance is

of the order of the main stream velocity. Therefore, the model assumption of negligible deviation from streamlines is not very realistic. The transport regime should be identified as mixed turbulent diffusion-inertial impaction. The present model does not account for inertial impaction of particles. A particle trajectory model must be used to calculate the contribution from that mechanism.

It is interesting to study the variation of deposition velocity with particle diameter. Figure 9 shows the variation at the leading edge, transition points and trailing edge. The model calculates infinite deposition rate at the exact leading edge. Therefore, results for the second computation stations on both surfaces are presented in Figure 9. For convenience these stations will be referred to as the "leading edge". On both sides of the blade nose, the deposition velocity decreases linearly (on the log-log scale) as diameter increases. The linearity starts

disappearing at d_p 0.1 μm beyond which direct inertial collection becomes important. The appropriate transport regimes are as indicated in the figure. If account were taken of direct inertial collection by means of a trajectory model, the curves would undergo a minimum (in the mixed Brownian diffusion-inertial impaction regime) and would increase with further increase in size.

The elbow shaped curves in Figure 9 display the variation of deposition velocity with particle diameter at the transition and trailing edge points. Based on the previous discussions, the approximate ranges of transport regimes are as indicated. Suction surface deposition rate is higher at transition (higher velocity and smaller boundary layer thickness). The opposite is true at the trailing edge (same velocity, greater thickness). For the same reasons, turbulent diffusion actually breaks in earlier on suction surface than on pressure surface, but later at the trailing edge. The change in slopes at the start of the mixed turbulent diffusion-inertial impaction regime is noteworthy. At the risk of being repetitive, the authors would like to caution the reader once again that the contribution

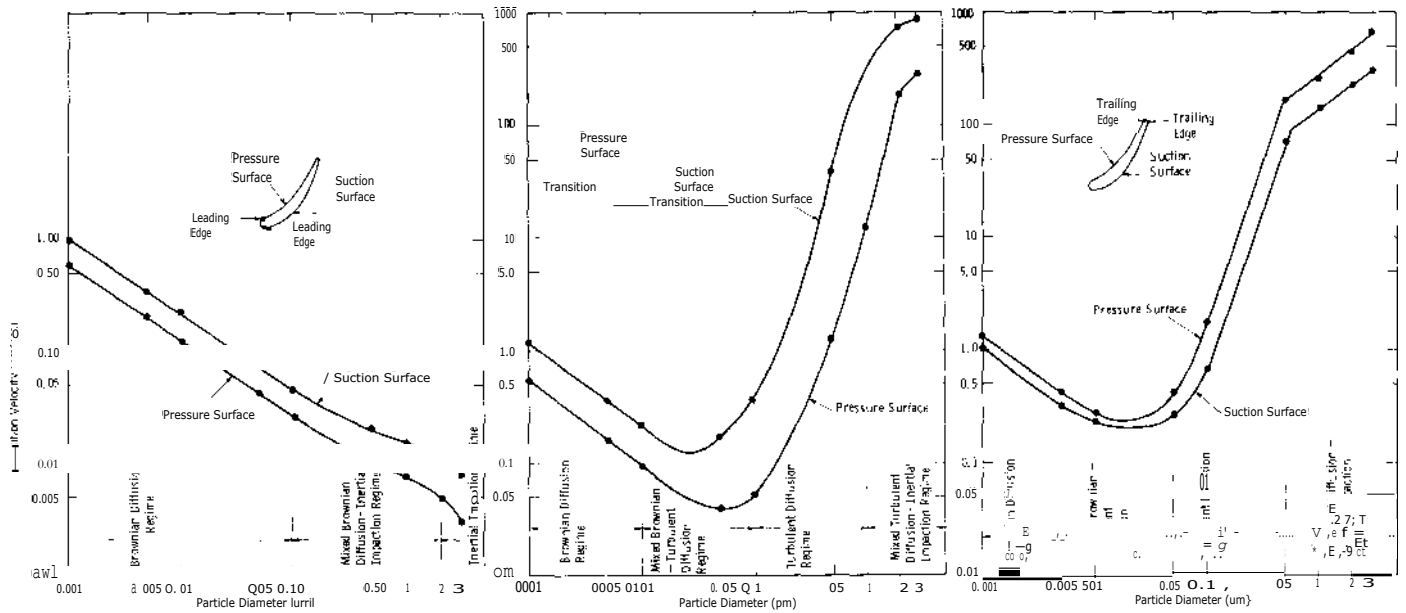


Fig. 9 Deposition velocities at stator blade leading edge, transition and trailing edge as a function of particle diameter

due to purely inertial mechanism is to be calculated by a separate particle trajectory model. It is important to note that this contribution may be positive or negative depending on the surface orientation. With reference to the mixed turbulent diffusion-inertial impaction regime in Figure 9, suction surface deposition rates should be lower at the trailing edge than predicted here, but pressure surface rates should be higher.

Deposition In a Gas Turbine Stage

This calculation procedure for determining the submicron arrival rates can be used to estimate deposition in a gas turbine stage - if the particle size distribution which the turbine is ingesting is known and if some assumption is made concerning the fraction of the arriving particles that will stick to the surface.

In this section, to illustrate the procedure and to provide a first estimate of the gas cleaning requirements to avoid deposition problems in a turbine expanding a gas containing large quantities of sub-micron particles, we estimate the growth of deposits and the effect of the deposits on turbine performance.

Figure 10 shows the particle size distribution we have selected for illustration. Fifty weight percent of the particles are larger than 1.3 microns. The distribution is an approximation of that which might be expected to leave a fabric filter. We have assumed the particulate concentration at the entrance to the turbine stage to be 0.002 grains per standard cubic foot (5 milligrams per standard cubic meter).

The deposition rates in the turbine stage were obtained by a stepwise integration of the deposition of each particle size over the range of particle sizes entering the turbine. It was assumed that all particles smaller than 3 μ m diameter stick to the surface and form homogeneous layers of deposit, but larger

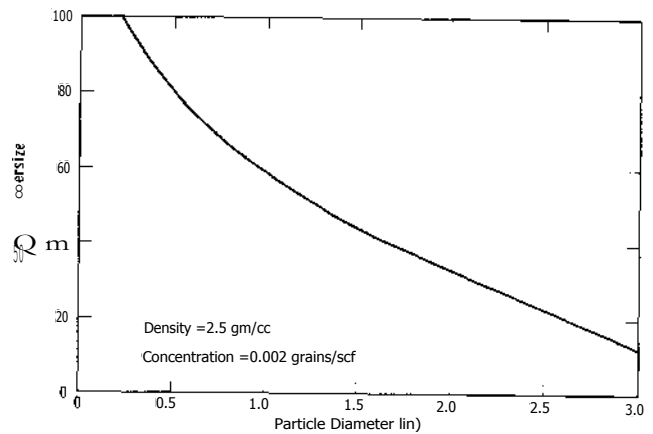


Fig. 10 Particle data used in deposition calculations

particles just impact the surface and rebound into the main stream owing to their high kinetic energy. In other words, the sticking probability was taken to be 100 % for 3 μ m and smaller particles, and 0.1 for larger particles.

Figure 11 shows the calculated thickness of deposits on the first stage stator and rotor blades after 250 hours of operation for this particle distribution entering the stage. The resulting change in the blade profiles and the blockage of the flow passage are illustrated in Figure 12. The authors feel that the thick deposit layers predicted near the noses are not realistic. The gas flow will actually break up the deposits in these regions long before the blade profiles are distorted to the extent shown in the figure.

The effect of the deposition on the stage performance was studied by considering the flow blockage

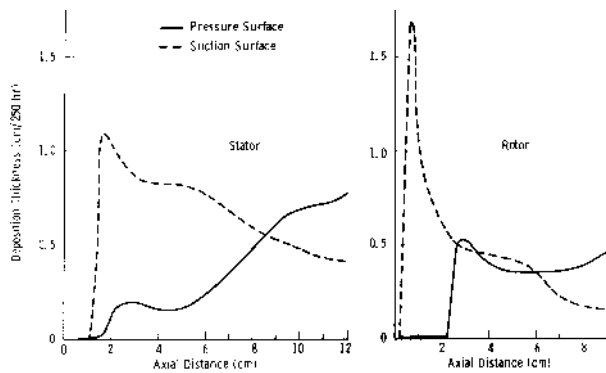


Fig. 11 Calculated deposition thicknesses on stator and rotor blades after 250 hr operation

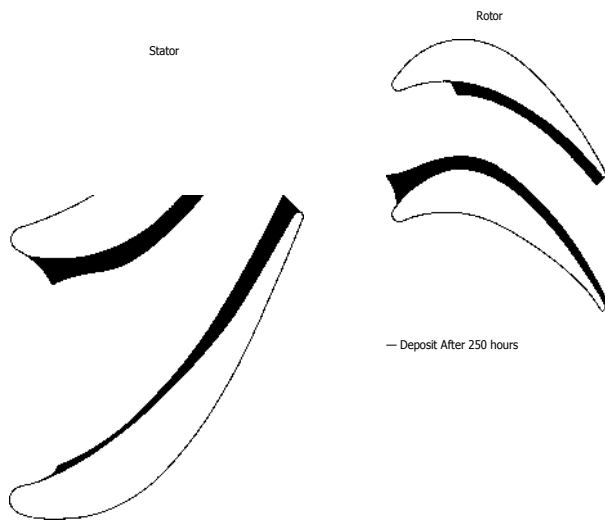


Fig. 12 Deposition in the first stage

at the nozzle throat and the profile and trailing edge losses due to the deposits. It was assumed that the deposits around the blade noses would be constantly removed by the gas flow so that they would have negligible effect on the stage performance. Figure 13 shows the estimated loss in the stage output power. The stage is estimated to lose about 20 % of its power in 150 hours of operation.

The deposition experience with a smaller 15 MW gas turbine unit reported by Nakao et al. [20] indicates that their turbine had to be cleaned after the power output dropped by approximately 4 F. Applying the same criterion for the 70 MW turbine under consideration, it is estimated that the turbine cleaning will be needed every 30 hours of operation when all arriving particles smaller than three microns contribute to the deposit. Only about 15 % of the deposit thickness results from the submicron particles. If 90 % of the deposit was subsequently removed and if particles larger than one micron would bounce off the surface - the time before cleaning was required would be extended by a factor of roughly fifty to one hundred

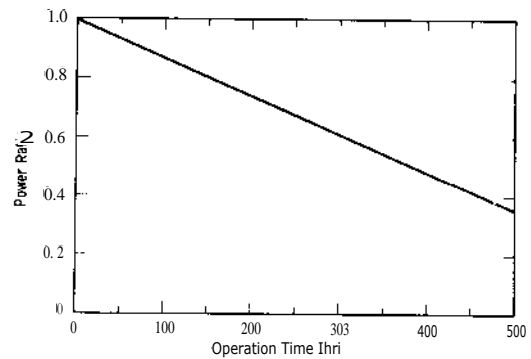


Fig. 13 Effect of deposition on power output of stage

times.

Accurate data on particle sticking fraction is required. Further research is recommended to study mechanisms of particle attachment to surfaces by theoretical and experimental means so that a reasonable estimate of sticking probability could be achieved. Observations by many investigators (e.g. See Kline, et al [21]) revealed that the laminar sublayer in a turbulent boundary layer flow is not entirely free from turbulence. The sublayer is subjected to occasional bursts of fluid being ejected from very close to the wall well into the turbulent core. Deposits can be removed due to these eruptions in the sublayer. The net deposition rates should be obtained by extending the analysis presented in this paper by including the particle attachment-detachment mechanisms and re-entrainment.

Thermophoresis is not considered here. Vermes [22] has pointed out that when the particle size distribution which the turbine is ingesting has a considerable mass of particles in the size range, having diameters of hundredths to tenths of a micron, and if the turbine employs cooled blading, thermophoresis will increase the delivery of these fine particles to blade surfaces and should be considered. In the application considered in this work - the possible deposition problems faced by a turbine expanding a particle distribution having a mass mean diameter of one micron - such as might be present in gases from fluidized or entrained bed coal gasification systems with hot gas clean-up - the contribution of thermophoresis to fine particle arrival rates will be small. As pointed out by Mr. Vermes, in conventional oil or gas fueled turbines or in turbines combusting residual fuel - the particulate distributions ingested by the machine have mass mean diameters in the critical range where additional deposition by thermophoresis will occur.

REFERENCES

- 1 Einstein, A., Theory of Brownian Motion, E.P. Dutton Co.
- 2 Parker, G.J., and Lee, P., "Studies of the Deposition of Submicron Particles on Turbine Blades", Proc. Inst. Mech. Engrs., Vol. 186, No. 38, 1972.
- 3 Lin, C.S., Moulton, R.W., and Putnam, G.L., "Mass Transfer Between Solid Wall and Fluid Streams", Ind. and Engr. Chem., Vol. 45, No. 3, 1953.

- 4 Moore, M.J., and Crane, R.I., "Aerodynamic Aspects of Gas Turbine Blade Corrosion", Deposition and Corrosion in Gas Turbines, edited by Hart, A.B., and Cutler, A.J.B., Ch. 4, John Wiley and Sons, 1973.
- 5 Crane, R.I., "Deposition of Fog Drops on Low Pressure Steam Turbine Blades", J. Mech. Sci., Vol.15, 1973.
- 6 Welty, J.R., Wicks, C.E., and Wilson, R.E., Fundamentals of Momentum, Heat and Mass Transfer, John Wiley and Sons, 1969.
- 7 Liu, B.Y.H., and Ilori, T.A., "Aerosol Deposition in Turbulent Pipe Flow", Env. Sci. and Tech., Vol. 8, No. 4, 1974.
- 8 Van Driest, E.R., "On Turbulent Flow Near a Wall", J.A.S., Vol. 23, No. 11, 1956.
- 9 Cebeci, T., Smith, A.M.O., and Wang, L.C., "A Finite-Difference Method for Calculating Compressible Laminar and Turbulent Boundary Layers", Donnel Douglas Aircraft Company, Report No. DAC-67131, Parts 1 and 2, 1969.
- 10 Klebanoff, P.S., "Characteristics of Turbulence in a Boundary Layer with Zero Pressure Gradient", NACA TN 3178, 1954.
- 11 Hayes, W.D., and Probst, R.F., Hypersonic Flow Theory, Academic Press, New York, 1959.
- 12 Friedlander, S.K., and Johnstone, H.F., "Deposition of Suspended Particles from Turbulent Gas Streams", Ind. and Engr. Chem., Vol. 49, No. 7, 1957.
- 13 Davies, C.N., "Deposition from Moving Aerosols" Aerosol Science, New York, 1966.
- 14 Beal, S.K., "Deposition of Particles in Turbulent Flow on Channel or Pipe Walls", Nucl. Sci. and Engr., 40, 1970.
- 15 Wells, A.C., and Chamberlain, A.C., G. Brt. J. Appl. Phys., Vol. 18, No. 12, 1967, pp. 1793-9.
- 16 Parker, and Ryley, D.J., "Equipment and Techniques for Studying the Deposition of Submicron Particles on Turbine Blades", Proc. Instn. Mech. Engr., 184(Pt3C) 45, 1969-70.
- 17 Katsanis, T., "Fortran Program for Calculating Transonic Velocities on a Blade-to-Blade Stream Surface of a Turbomachine", NASA T.D. No. 5427, 1969.
- 18 Horlock, J.H., Flow Research on Blading, Ed. by Dzung, L.S., Amsterdam, Elsevier, 1970.
- 19 MengiitDrk, M., and Sverdrup, E.F., "Calculated Tolerance of a Large Electric Utility Gas Turbine to Erosion Damage by Coal Gas Ash Particles", Erosion: Prevention and Useful Applications, ASTM STP 664, Ed. by Adler, W.F., 1979.
- 20 Nakao, K., Hirai, H., and Omori, T., "Two Years Experience of a Gas Turbine Firing Residual Fuel", ASME, 68-6T-11.
- 21 Kline, S.J., Reynolds, W.C., Schraub, F.A., and Runstadler, P.W., "The Structure of Turbulent Boundary Layers", J. Fluid Mech., Vol. 30, No. 4, 1967.
- 22 Vermes, G., "Thermophoresis - Enhanced Deposition Rates in Combustion Turbine Blade Passages", ASME paper 78-WA/GT-1, 1978.